

## CONTEXT-AWARE LOCAL PLANNING FOR PERSONAL CARE ROBOTS

GUANG YANG AND SHUOYU WANG

School of Systems Engineering  
Kochi University of Technology  
185 Miyanokuchi, Tosayamada, Kami City, Kochi 782-8502, Japan  
218004i@gs.kochi-tech.ac.jp; wang.shuoyu@kochi-tech.ac.jp

Received April 2019; revised August 2019

**ABSTRACT.** *Human caregivers can provide high-quality caring services because their behavior considers where they are and what/who is around them. For a personal care robot to provide caring services similarly, a context-aware local planning method is presented that allows a robot to change between different operating patterns at run time. With a control system that integrates the proposed method, a personal care robot can behave based on the type of room in which it currently stands and whether there are people within its operating range. The proposed method has been tested in an actual household environment and was proved to be effective.*

**Keywords:** Context awareness, Personal care, Local planner, Dynamic window approach

1. **Introduction.** Personal care robots can help with the everyday activities of people who suffer from illness, disease, or injury. A fine-tuned local planner is essential for a robot to follow a planned path while avoiding obstacles. Within this well-studied domain, our area of interest is a local planner that can change its configurations actively considering the environmental context.

In the field of robotics, context awareness refers to the ability of a robot to sense and react according to its environment [1,2]. A semantic-aware robotic system typically comprises two functions, namely (i) recognizing different environmental semantics and (ii) reacting accordingly with reasonable actions. In the present work, we focus on the latter function.

Previous research has introduced context-aware global planning methods that allow a robot to plan a global path without invading human workspaces [3]. However, in scenarios involving homecare in household environments, interacting closely with people is inevitable. Because avoiding certain locations is not an option, we argue that a context-aware local planner is required for the robot to deal with diverse scenarios.

The need for a context-aware local planner can be explained with a simple caring scenario involving a human caregiver. While caring for a bedridden patient, the caregiver walks relatively quickly through doorways and empty rooms (i.e., where there are no other people). However, upon entering the bedroom, the caregiver slows down so as not to disturb the patient. Furthermore, when conducting activities near the patient or other people, the caregiver pays extra attention so as to avoid accidents such as colliding with people or dropping objects. Put simply, a human caregiver performs homecare tasks with different behavioral characteristics depending on where she/he is and who/what is around.

Herein, we first present a dynamic re-configurable local planner so that suitable behavioral characteristics can be triggered with pre-defined semantic labels. We then introduce a complete system describing how a robot can take advantage of the proposed planner. Finally, through extensive experiments in an actual household domain, we establish that the proposed approach is effective.

**2. Related Work.** Semantic information can provide considerable impetus for advances in robotics applications, especially when considering human environments. Researchers have previously built a system based on a state-of-the-art convolutional network, generating semantic labels for indoor (e.g., kitchen, office, corridor) and outdoor (e.g., parking garage, food court, café) environments [4]. Meanwhile, a method for representing and modeling indoor affordance areas based on the codebookless model (CLM) has been proposed that classifies indoor affordance areas for service robots [5].

With the means to sense or predict semantic information in an operating environment, considerable corresponding efforts have been made to enable robot motion that is more reasonable and effective, the main direction being semantic-aware path planning. Human motion patterns have been learned based on sampled hidden Markov models and used in a path-planning algorithm based on a probabilistic roadmap [3]. This was done to minimize social distractions such as going through someone's working space. From another perspective, avoiding the need to observe people, an affordance map has been proposed that describes the environment considering geometric features, whereupon a global planning method A\* could be conducted aimed at a semantic-aware global path [1]. With such global paths generated, robots can operate considering humans' requirements rather than only geometry constraints.

The aforementioned approaches are focused on minimizing the extent to which robots affect people by preventing the former from entering the working spaces of the latter. However, to provide personal care services, entering the working spaces of the patients is typically unavoidable. Also, in contrast to the global planning, to the best of our knowledge, re-configuring a local planner [6] in run time to achieve better performance is yet to be discussed.

**3. Context-Aware Local Planning Method.** In this section, we introduce a robot controller based on a dynamic window approach (DWA). We also discuss how we modified the original approach to be able to adjust the robot motion given a pre-defined semantic label.

**3.1. Platform configuration.** Figure 1 shows our personal care robot KUT-PCR [7], where the schematic on the left shows the front-back configuration of two laser range finders. With a scan range of  $135^\circ$  for a single sensor, the robot has a  $360^\circ$  perception of its surroundings. This provides a robust source of data for applications including (i) simultaneous localization and mapping (SLAM) and (ii) obstacle avoidance.

The schematic on the right of Figure 1 shows the workspace of the upper body. As a result of a highly flexible upper body, the workspace is clearly larger than the mobile platform.

**3.2. Dynamic footprint.** The DWA generates actuator commands so that the robot can follow the global path without running into obstacles or violating the dynamic limitations of the actuators. An initial step is to define the footprint of the robot with a polygon, which is the basis for collision checking in the following procedures. In most cases, the footprint is hardcoded and remains unchanged unless there is a mechanical re-design.

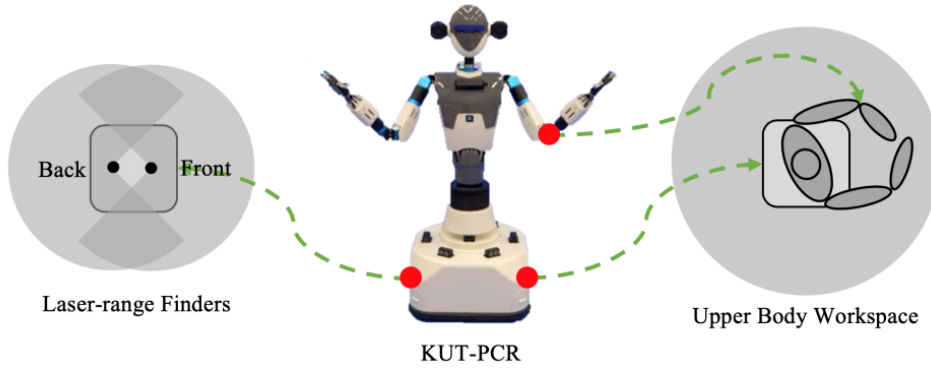


FIGURE 1. Personal care robot KUT-PCR

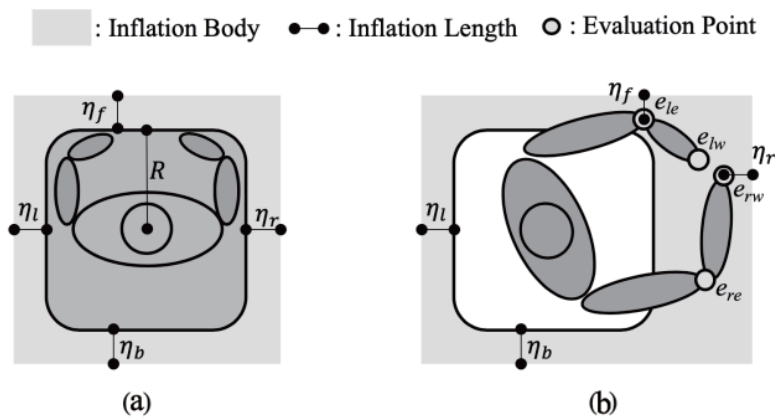


FIGURE 2. Dynamic footprint

In our implementation, the robot footprint is assumed to be dynamic with two considerations, namely that (i) different levels of safety should be achievable by adjusting the size of the footprint and (ii) for a mobile humanoid robot, the configurations of the upper body should also be considered for controlling the motion of the mobile platform.

Figure 2(a) shows the upper body remaining within the mobile platform; the light-black area is referred to as the inflation footprint, obtained by extending the robot shape in four directions with the inflation lengths  $\eta_f$ ,  $\eta_l$ ,  $\eta_b$ , and  $\eta_r$ . The original footprint considering only the mobile platform without inflation is a square of side  $2R$ , while an actual footprint is described by the distances from the origin to each side. Therefore, the expanded footprint in Figure 2(a) is denoted as  $\mathbf{F} = \{R + \eta_f, R + \eta_l, R + \eta_b, R + \eta_r\}$ . The inflation provides a “safe zone” between obstacles and the robot. A larger inflation body provides better capability to deal with possible collisions, such as those with fast-moving obstacles.

In Figure 2(b), the forearms of the upper body reach beyond the mobile platform, therefore requiring a method for expanding the footprint considering the upper-body configuration. Evaluation points  $e_{le}$ ,  $e_{lw}$ ,  $e_{re}$ , and  $e_{rw}$  represent the coordinates mapped to the ground of the robot’s left elbow joint, left wrist, right elbow joint, and right wrist, respectively.

Table 1 presents a footprint inflation algorithm that calculates the expanded footprint on the fly with respect to the evaluation points on the upper body. First, a footprint  $\mathbf{F}$  considering only the mobile platform is initialized. The evaluation points are then passed to the function *CALC\_RECTANGLE* that calculates the minimum bounding rectangle

TABLE 1. Footprint inflation algorithm

---

**Algorithm:** INFLATION

---

**Input:** Evaluation points  $e_{le}$ ,  $e_{lw}$ ,  $e_{re}$ , and  $e_{rw}$

**Output:** Expanded footprint  $F$

// Initialize a footprint.

$$F = \{R + \eta_f, R + \eta_l, R + \eta_b, R + \eta_r\}$$

// Calculate the minimum bounding rectangle from the evaluation points.

$$REC = \text{CALC\_RECTANGLE}(e_{le}, e_{lw}, e_{re}, e_{rw})$$

// Evaluate each distance in the generated rectangle.

**for**  $i = 1$  to 4 **do**

**if**  $REC[i] > R$  **then**

$F[i] = REC[i]$

**end if**

**end for**

**return**  $F$

---

$REC$  of the input point sets by using the gift-wrapping method. We then evaluate each distance (origin to side distance) in  $REC$  with  $R$ ; if the distance exceeds  $R$ , then the corresponding distance in  $F$  is replaced. Eventually, the resulting footprint is returned.

**3.3. Additional reduction of velocity search space.** KUT-PCR sits on an omnidirectional mobile platform: transitional/rotational motion is generated by four omnidirectional wheels and is denoted as  $v(\dot{x}, \dot{y}, \dot{\theta})$ . Normally, the search space of the possible velocities is reduced as follows.

**3.3.1. Circular trajectories.** The DWA considers only circular trajectories, which are determined by a given velocity comprising the two-dimensional translational speed  $(\dot{x}, \dot{y})$  and the one-dimensional rotational speed  $\dot{\theta}$ . This leads eventually to a three-dimensional velocity search space (Figure 3(a)). For clarity, we discuss the problem in a two-dimensional space considering only  $\dot{x}$  and  $\dot{\theta}$  (Figure 3(b)). Initially, the space  $V_s$  is determined by the actuator limitations (maximum and minimum speed).

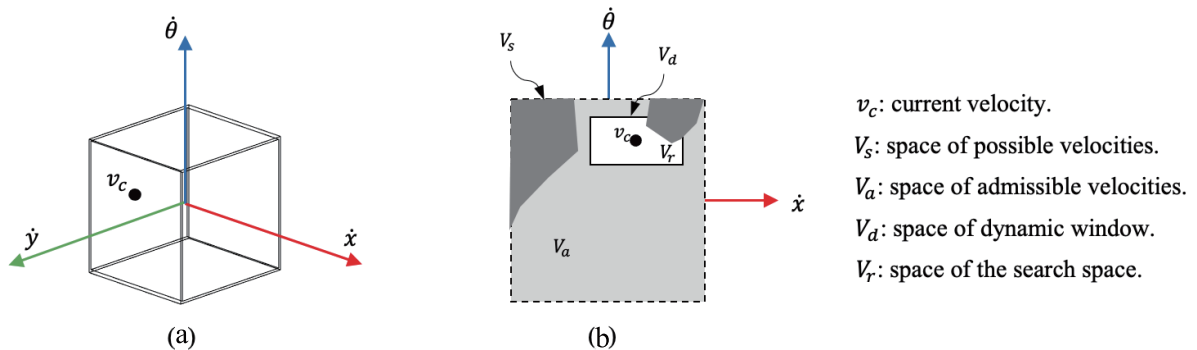


FIGURE 3. Velocity search space

**3.3.2. Admissible velocities.** Avoiding obstacles is the top priority for a robot. Any generated circular trajectory that could result in colliding with an obstacle is considered a failed trajectory and the corresponding velocity is regarded as inadmissible. All the safe trajectories in the initial space establish a space  $V_a$ .

3.3.3. *Dynamic window.* Originally, the dynamic window  $V_d$  contains the velocities that are reachable in the next time interval, considering the limited accelerations of the actuators. Thus, the final velocity search space  $V_r$  is calculated as

$$V_r = V_s \cap V_a \cap V_d. \tag{1}$$

In our application, we assume that reducing the dynamic window and initial velocity space further results in different motion patterns fitting certain requirements.

3.3.4. *Reduction of  $V_s$ .* Usually, robots tend to exhaust the power of the actuators to obtain the highest performance (greatest efficiency). However, in personal care scenarios, there can be additional restriction on the actuators. In Figure 4(a), we reduce the rotational speed equally in both directions to avoid high-speed turning actions. The translational speed in the forward direction is similarly limited, whereas the limitation on the backward direction is obviously larger. This indicates that although the backward speed is required to avoid dynamic obstacles, high-speed backward operation in a human-centered environment is dangerous. The reduction  $\zeta_s$  is denoted as

$$\zeta_s = \left\{ \dot{x}_{\max}, \dot{x}_{\min}, \dot{y}_{\max}, \dot{y}_{\min}, \dot{\theta}_{\max}, \dot{\theta}_{\min} \right\}, \tag{2}$$

where  $\dot{x}_{\max}$ ,  $\dot{x}_{\min}$  are the velocity limitations in the positive and negative directions, respectively, on the  $x$  axis, and  $\dot{y}_{\max}$ ,  $\dot{y}_{\min}$ ,  $\dot{\theta}_{\max}$ ,  $\dot{\theta}_{\min}$  are the restrictions on the  $y$  and  $\theta$  axes, respectively.

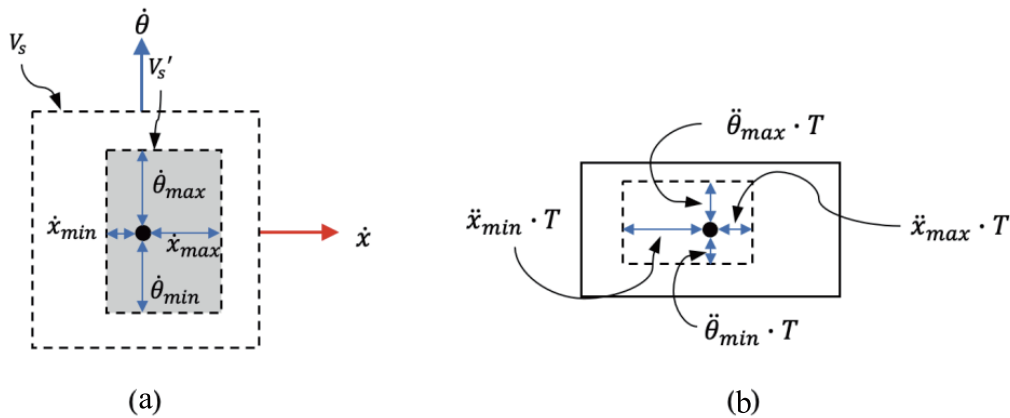


FIGURE 4. Additional limitation on velocity search space

3.3.5. *Reduction of  $V_d$ .* While  $V_s$  defines the operation bounds, the dynamic performance considering acceleration/breaking is determined by  $V_d$ . The original dynamic window  $V_d$  is typically a rectangle located symmetrically around the current speed, but we add an additional limitation for further reduction. For instance, although high-speed backward operation must be prohibited, we expect backward motion while avoiding a dynamic obstacle to be efficient (i.e., with high acceleration). The reduction of  $V_d$  is described with  $\zeta_d$ , namely

$$\zeta_d = \left\{ \ddot{x}_{\max}, \ddot{x}_{\min}, \ddot{y}_{\max}, \ddot{y}_{\min}, \ddot{\theta}_{\max}, \ddot{\theta}_{\min} \right\}, \tag{3}$$

where  $\ddot{x}_{\max}$  and  $\ddot{x}_{\min}$  are the acceleration limits in the positive and negative directions, respectively, of accelerations  $\ddot{x}$ ,  $\ddot{y}_{\max}$ ,  $\ddot{y}_{\min}$ ,  $\ddot{\theta}_{\max}$ , and  $\ddot{\theta}_{\min}$  are the limitations of accelerations  $\ddot{y}$  and  $\ddot{\theta}$ , respectively, and  $T$  is the time interval (Figure 4(b)). By tuning parameters  $\eta_f$ ,  $\eta_b$ ,  $\eta_l$ ,  $\eta_r$ ,  $\zeta_s$ , and  $\zeta_d$ , different behavioral patterns of the robot can be defined freely.

**3.4. Semantic controller configurations.** Now that the controller has been configured to be adjustable considering efficiency, safety, or motion preference, a method is required for matching the configurations with semantic information. In this work, we classify the semantic labels into two groups, namely spatially dependent labels and object-dependent labels. Spatially dependent labels refer to locations such as kitchen, bedroom, doorway, whereas object-dependent labels are triggered when the robot detects certain objects, including the patient being taken care of or other individuals. The  $i$ th behavior pattern  $P_i$  is defined with the  $m$ th semantic label  $L_m$  and the corresponding  $n$ th pre-defined planner configuration  $conf_n$ , namely

$$P_i = (L_m, conf_n). \quad (4)$$

**4. System Configuration.** We now introduce a complete system (Figure 5) that enables a personal care robot to reconfigure the local planner dynamically considering environmental semantics. The dark blocks refer to the modules introduced herein, while the light ones are robot-specific software packages. Block 1 comprises navigation and object-detection functions; the module perceives the environment continuously and passes semantic labels to block 3 if certain locations are reached or objects are detected. Block 3 keeps a list of all the pre-defined patterns; given a semantic label, it simply goes through all the patterns and chooses the configuration corresponding to the given semantic label. Meanwhile, the checking points sent from block 2 are evaluated by block 4, deciding how the footprint should be adjusted. Blocks 3 and 4 both produce planner parameters that are then sent to block 5. In the system, the communication between blocks 5 and 6 takes place at 10 Hz, while the rest are event-driven with no fixed updating frequency.

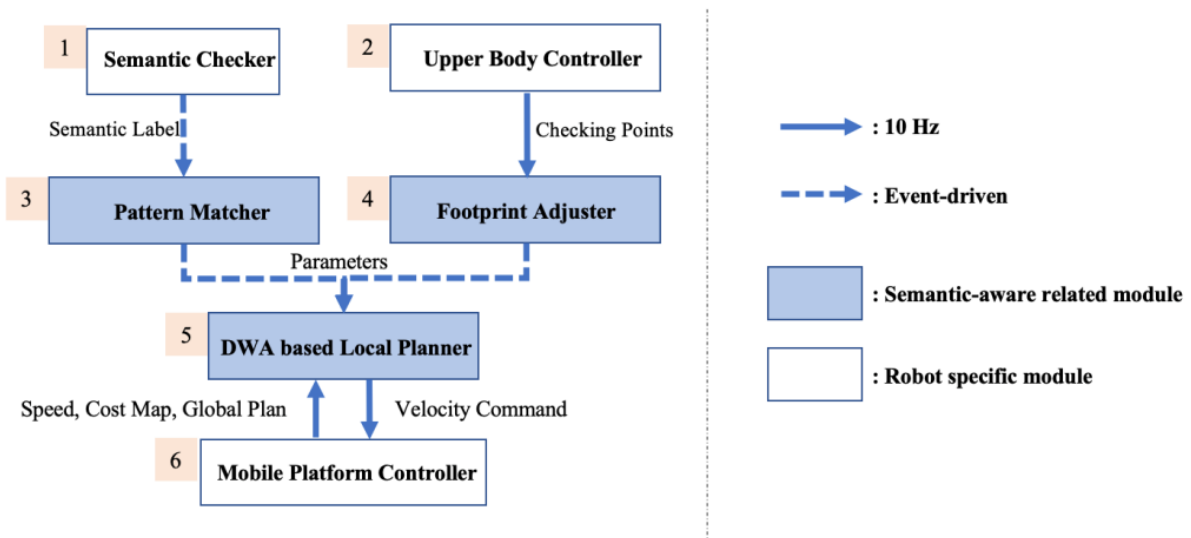


FIGURE 5. Control system diagram

**5. Experiments and Results.** To evaluate the proposed method, we conducted experiments in an actual household environment. In the first experiment, we examined how the dynamic footprint guaranteed safety during operations of a humanoid mobile platform. In the scenario, KUT-PCR was expected to fetch objects from the refrigerator and deliver them to the next-door room. In trial 1, the robot did not pick up anything. In trial 2, the robot picked up a bottle of drink; it held the bottle with two arms stretched out.

As Figure 6 shows, in trial 1 the upper body stayed within the range of the mobile platform, thus the robot finished the task having strictly followed the global path. In

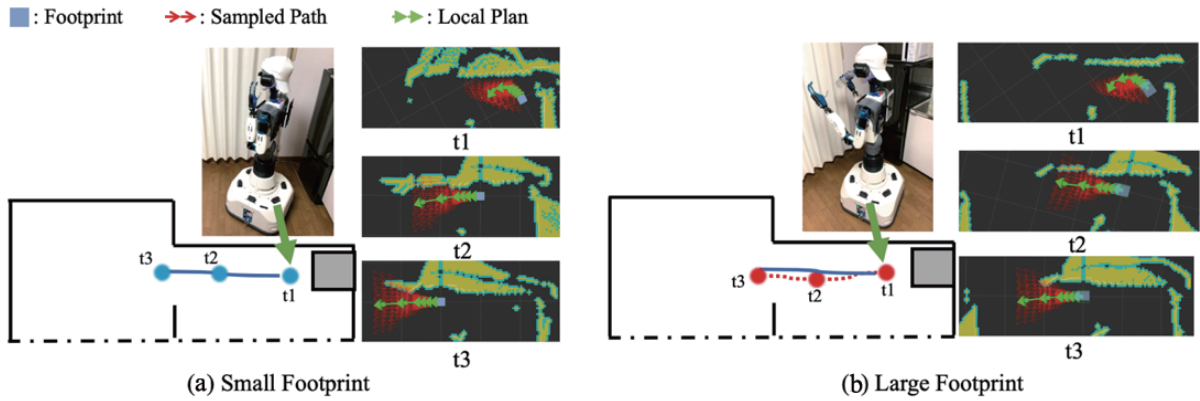


FIGURE 6. Experimental trials without and with dynamic footprint

Pattern ID	Name	Footprint Size	vel_x forward	vel_x backward	vel_y	vel_w	acc_x	acc_y	acc_w
1	Kitchen	■■■■	■■■■■	■	■■■	■■■	■■■■	■■■	■■■■■
2	Bedroom	■■■■■	■■■	■	■■■	■	■■■■	■■■	■■■■■
3	Doorway	■	■■	■	■■	■	■■■■	■■■	■■
4	Near Patient	■■	■	■	■	■	■■■■	■■■	■■■

■ : Very Small   ■■ : Small   ■■■ : Middle   ■■■■ : Big   ■■■■■ : Very Big

FIGURE 7. Behavioral pattern configurations

trial 2, with the arms stretched outside the mobile platform, the dynamic footprint method kept the robot away from the wall with a path that departed slightly from the planned global path.

In the second experiment, we conducted a fetch-and-serve task commonly seen during caring services and we examined how the behavioral patterns of the robot changed when faced with different semantic situations. Figure 7 demonstrates the parameter configurations of four behavioral patterns including “Kitchen”, “Bedroom”, “Doorway”, and “Near Patient”. Parameters considering footprint size, velocity in the direction of  $x$  axis and  $y$  axis ( $vel_x$ ,  $vel_y$ ), rotational velocity ( $vel_w$ ), acceleration in the direction of  $x$  axis and  $y$  axis ( $acc_x$ ,  $acc_y$ ), and rotational acceleration ( $acc_w$ ) are described with five levels: very small, small, middle, big, and very big.

As shown in Figure 8, at  $t_1$ ,  $t_2$ , and  $t_3$  the robot detected semantic locations (“Doorway”, “Bedroom”, and “Kitchen”); at  $t_4$  the object-dependent semantic label “Near patient” was triggered. The robot succeeded in switching among four pre-defined behavioral patterns dealing with different semantic scenarios. The parameters served the purpose of achieving various operation patterns; however, the specific parameter values that each pattern corresponds can be adjusted freely to meet diverse requirements.

**6. Conclusions.** In this paper, we introduced a context-aware local planning method for personal care robots. A strategy was presented for dynamic footprint adjustment to guarantee safe operation considering the upper body of a mobile humanoid robot. We then presented a dynamic adjustable local planner that allows real-time behavior switching considering semantic labels. These methods can be integrated into a robot system to enable semantic-aware behaviors, which we evaluated in our personal care robot in an actual household environment. Nevertheless, the present method relies on human experience to test out suitable parameters for achieving certain behavioral patterns. In

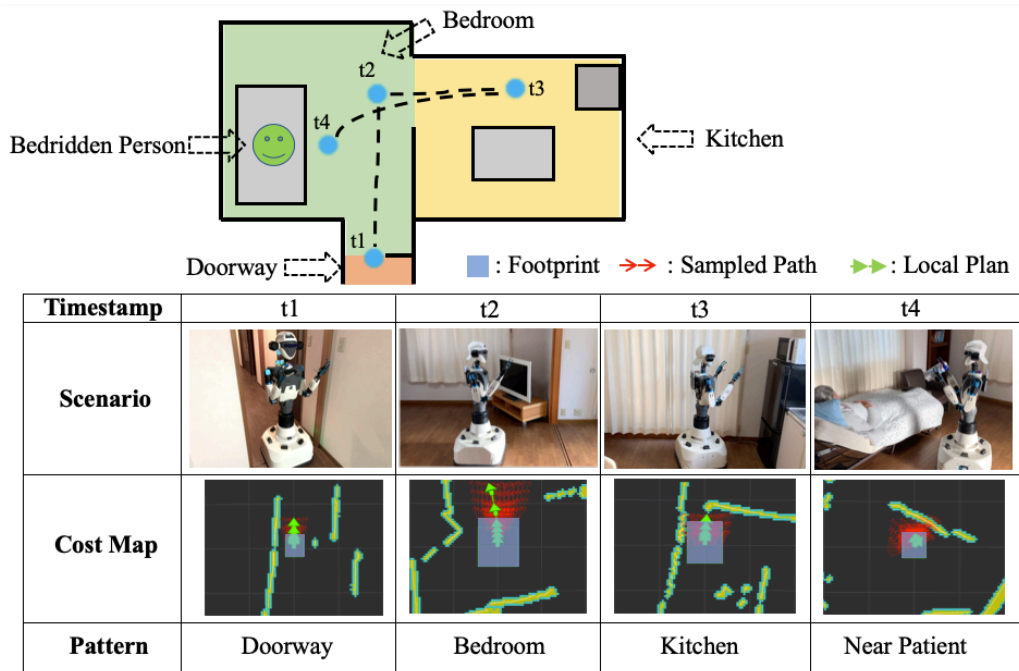


FIGURE 8. Personal care trial considering environmental context

future work, we intend to build more-intelligent systems to generate suitable planner parameters considering given semantic information.

**Acknowledgments.** This work was supported by JSPS KAKENHI Grant No. 15H03951, the Canon Foundation, and the Casio Science Promotion Foundation.

#### REFERENCES

- [1] L. Piyathilaka and S. Kodagoda, Affordance-map: A map for context-aware path planning, *Proc. of Australasian Conference on Robotics and Automation*, Melbourne, 2014.
- [2] W. Budiharto and C. Ishii, Coffee maker robot based on simple vocabulary and partially observable Markov decision process (POMDP), *ICIC Express Letters*, vol.11, no.4, pp.757-762, 2017.
- [3] S. Sehestedt, S. Kodagoda and G. Dissanayake, Robot path planning in a social context, *Proc. of IEEE Conference on Robotics, Automation and Mechatronics*, pp.206-211, 2010.
- [4] N. Süderhauf, F. Dayoub, S. McMahon et al., Place categorization and semantic mapping on a mobile robot, *Proc. of IEEE International Conference on Robotics and Automation*, pp.5729-5736, 2016.
- [5] P. Wu, Y. Li, F. Yang, L. Kong and Z. Hou, A CLM-based method of indoor affordance areas classification for service robots, *Robot*, vol.40, no.2, pp.188-194, 2018.
- [6] D. Fox, W. Burgard and S. Thrun, The dynamic window approach to collision avoidance, *IEEE Robotics & Automation Magazine*, vol.4, no.1, pp.137-146, 2016.
- [7] G. Yang, S. Wang, J. Yang, B. Shen and P. Shi, Pose estimation of daily containers for a life-support robot, *International Journal of Innovative Computing, Information and Control*, vol.14, no.4, pp.1545-1552, 2018.